



HHS Public Access

Author manuscript

Brain Res. Author manuscript; available in PMC 2020 November 01.

Published in final edited form as:

Brain Res. 2019 November 01; 1722: 146349. doi:10.1016/j.brainres.2019.146349.

Diverse Glutamatergic Inputs Target Spines Expressing M1 Muscarinic Receptors in the Basolateral Amygdala: An Ultrastructural Analysis

Alexander J. McDonald*, Grace C. Jones, David D. Mott

Department of Pharmacology, Physiology and Neuroscience University of South Carolina School of Medicine Columbia, SC, USA.

Abstract

Although it is known that acetylcholine acting through M1 muscarinic receptors (M1Rs) is essential for memory consolidation in the anterior basolateral nucleus of the amygdala (BLA), virtually nothing is known about the circuits involved. In the hippocampus M1R activation facilitates long-term potentiation (LTP) by potentiating NMDA glutamate receptor (NMDAR) currents. The majority of NMDAR+ profiles in the BLA are spines. Since about half of dendritic spines of BLA pyramidal neurons (PNs) receiving glutamatergic inputs are M1R-immunoreactive (M1R+) it is possible that the role of M1Rs in BLA mnemonic functions also involves potentiation of NMDAR currents in spines. However, the finding that only about half of BLA spines are M1R+ suggests that this proposed mechanism may only apply to a subset of glutamatergic inputs. As a first step in the identification of differential glutamatergic inputs to M1R+ spines in the BLA, the present electron microscopic study used antibodies to two different vesicular glutamate transporter proteins (VGluTs) to label two different subsets of glutamatergic inputs to M1R+ spines. These inputs are largely complimentary with VGluT1+ inputs arising mainly from cortical structures and the basolateral nucleus, and VGluT2+ inputs arising mainly from the thalamus. It was found that about one-half of the spines that were postsynaptic to VGluT1+ or VGluT2+ terminals were M1R+. In addition, a subset of the VGluT1+ or VGluT2+ axon terminals were M1R+, including those that synapsed with M1R+ spines. These results suggest that acetylcholine can modulate glutamatergic inputs to BLA spines by presynaptic as well as postsynaptic M1R-mediated mechanisms.

Keywords

amygdala; M1 muscarinic receptors; VGluT1; VGluT2; immunohistochemistry; electron microscopy

*Correspondence to: Alexander J. McDonald, Telephone: 803-216-3511 Fax: 803-216-3524, alexander.mcdonald@uscmed.sc.edu. Authors' contribution

Study concept and design: A.J.M. and D.D.M. Data acquisition: A.J.M. and G.C.J. Analysis and interpretation of data: A.J.M., G.C.J., D.D.M. Drafting of the manuscript: A.J.M. and D.D.M. Obtained funding: A.J.M. and D.D.M.

Publisher's Disclaimer: This is a PDF file of an unedited manuscript that has been accepted for publication. As a service to our customers we are providing this early version of the manuscript. The manuscript will undergo copyediting, typesetting, and review of the resulting proof before it is published in its final citable form. Please note that during the production process errors may be discovered which could affect the content, and all legal disclaimers that apply to the journal pertain.

Declarations of interest: none for all three authors

1. Introduction

The basolateral nuclear complex of the amygdala, especially the anterior subdivision of the basolateral nucleus proper (BLa), receives an extremely dense cholinergic innervation from the basal forebrain in both rodents (Mesulam et al., 1983a; Carlsen et al., 1985; Muller et al. 2011) and primates (Mesulam et al., 1983b; Kordower et al., 1989). Acetylcholine acting through muscarinic receptors is critical for memory consolidation by the BLa (Power et al., 2003a). Post-training infusions of muscarinic cholinergic antagonists into the BLa produce impairments in several types of emotional/motivational learning including fear conditioning and extinction, inhibitory avoidance, conditioned place preference, and drug-stimulus learning (Power et al., 2003a; Boccio et al., 2009). Although it is known that activation of both M1 and M2 muscarinic receptors (M1Rs and M2Rs) in the BLa is essential for memory consolidation functions performed by this nucleus, virtually nothing is known about the circuits that are involved (Power et al., 2003b).

M1Rs are also critical for mnemonic function in the hippocampus. It is well established that M1R activation facilitates long-term potentiation (LTP) in this region by potentiating NMDA glutamate receptor (NMDAR) currents (Markram and Segal, 1990; Shinoe et al., 2005; Buchanan and Mellor, 2010; Dennis et al., 2016). Dendritic spines in the hippocampus express NMDARs (Petralia et al., 1994), and there is colocalization of M1Rs and NMDARs in pyramidal neuron (PN) dendrites receiving glutamatergic inputs (Marino et al., 1998). In the BLa the great majority of spines arise from PN dendrites (McDonald, 1982; Millhouse and deOlmos, 1983). Since about half of dendritic spines of BLa PNs receiving glutamatergic inputs are M1R-immunoreactive (M1R+) (Muller et al., 2013), and the majority of NMDAR+ profiles in ultrastructural studies of BLa are spines (Farb et al., 1995), it is possible that the role of M1Rs in BLa mnemonic functions also involves potentiation of NMDAR currents in PN spines. However, the finding that only about half of BLa spines are M1R+ suggests that this proposed mechanism may only apply to a subset of glutamatergic inputs to BLa.

The BLa receives robust glutamatergic inputs from the cortex (including the hippocampus, entorhinal cortex, and prefrontal cortex) and the midline thalamus (Pitkänen, 2000; McDonald, 2019). As a first step in the identification of differential glutamatergic inputs to M1R+ spines in the BLa, the present electron microscopic study used antibodies to two different vesicular glutamate transporter proteins (VGluTs) to label two different subsets of glutamatergic inputs to M1R+ spines. These inputs are largely complimentary with VGluT1+ inputs arising mainly from cortical structures and the basolateral nucleus, and VGluT2+ inputs arising mainly from the thalamus (Fremeau et al., 2001; Kaneko and Fujjyama, 2002).

2. Results

2.1 Light microscopy

Light microscopic analysis of immunoperoxidase preparations using diaminobenzidine (DAB) as a chromogen revealed that VGluT1 and VGluT2 immunoreactivity in the BLa was

confined to small round or oval punctate structures that appear to correspond to the immunoreactive axons and axon terminals seen at the ultrastructural level (see below). Most of the VGluT1+ and VGluT2+ puncta were 0.5–1.0 μm in diameter, although some VGluT2+ puncta were slight larger (ca. 1.5 μm in diameter) (Figs. 1A and 1C). No cell bodies were VGluT1+ or VGluT2+. Light microscopic analysis of immunoperoxidase preparations using Vector Very Intense Purple (V-VIP) as a chromogen revealed M1R immunoreactivity in large somata that were the same size and shape as pyramidal neurons (PNs), consistent with previous studies of M1R immunoreactivity in the BLA (McDonald and Mascagni, 2010) (Fig. 1B). There was also diffuse M1R immunoreactivity in the neuropil at the light microscopic level of analysis.

2.2 Electron microscopy

At the electron microscopic level the V-VIP reaction product is particulate, and is easily distinguishable from the more diffuse reaction product of DAB (Figs. 2–4) (Van Haeften and Wouterlood, 2000). Particulate M1R immunoreactivity was seen in somata, dendrites, spines, axons, and axon terminals. DAB reaction product for VGluT1 and VGluT2 immunoreactivity was confined to axons and axon terminals. Reaction product in these terminals was concentrated along the membrane of synaptic vesicles, as expected for vesicular transporters.

The great majority of postsynaptic targets of axon terminals expressing VGluT1 or VGluT2 in the BLA were dendritic spines. However, some dendritic shafts were also targeted. All synapses were asymmetrical, typical of glutamatergic terminals. In both VGluT1 and VGluT2 preparations some of the targeted dendrites were M1R+ and some were M1R-negative. Approximately one-half of VGluT1+ and VGluT2+ axon terminals formed synapses with M1R+ spines (Table 1). In most spines the M1R+ immunoparticles either contacted or were in close proximity to postsynaptic densities (Figs. 2 and 3). Almost all M1R+ and M1R-negative spines were postsynaptic to one excitatory axon terminal, but one large spine received input from one VGluT2+ axon terminal and one unlabeled terminal that presumably was VGluT1+ (Fig. 3C).

Some VGluT1+ and VGluT2+ axon terminals contained M1R+ immunoparticles (Fig. 4). These M1R+ immunoparticles were only discernable in terminals with light DAB reaction product. Since the immunoparticles usually have dark exterior coats and lighter interiors, they are difficult to distinguish from synaptic vesicles in VGluT1+ and VGluT2+ axon terminals that are densely stained with DAB reaction product. In brain M-7, in which the VGluT1 and VGluT2 DAB reaction product was light and the M1R+ immunoparticles were densely stained it was found that more than one-quarter of both types of terminals were M1R+ (VGluT1: 28/92 [30.4%]; VGluT2: 26/93 [27.9%]). In brain M10, which had dense VGluT1 and VGluT2 reaction product, no double-labeled terminals were seen. In brain M12 16.7% (15/90) of VGluT1+ terminals and 2.4% (2/84) of VGluT2+ terminals were double-labeled. Collectively, about two-thirds of the spines targeted by VGluT1+/M1R+ double-labeled terminals (65.1%, 28/43) and 39.3% (11/28) of the spines targeted by VGluT2+/M1R+ double-labeled terminals were M1R+.

3. Discussion

3.1 Spines postsynaptic to VGluT1+ or VGluT2+ inputs express M1Rs: technical considerations

The main finding of this study is that M1R+ spines in the BLA are not targeted by one type of glutamatergic input, but instead by diverse glutamatergic inputs arising from either cortical or subcortical regions. Only one M1R+ spine (out of 529 M1R+ spines) was targeted by both a VGluT2+ excitatory terminal and an unlabeled (presumably VGluT1+) excitatory terminal. This suggests that thalamic and cortex/BLA terminals largely synapse with separate spines, consistent with studies by Lüthi and coworkers (Humeau et al., 2005).

This is the first electron microscopic (EM) study of VGluT1+ or VGluT2+ axon terminals and their targets in the basolateral amygdala. The percentages of M1R+ spines with VGluT1+ or VGluT2+ inputs obtained in this study are underestimates of the true percentages since the single thin-section analyzed may miss immunoparticles in the same spine in adjacent thin-sections (i.e., a false negative). The M1R antibody used in this study is specific for the m1 muscarinic receptor (see below) and has been used effectively in EM DAB-immunoperoxidase studies of the subcellular localization of this receptor in the cerebral cortex (Mrzljak et al., 1993), striatum (Hersch et al., 1994), and hippocampus (Rouse et al., 1998). Although immunogold EM techniques generally provide better spatial resolution of receptors, these DAB-immunoperoxidase studies demonstrated very good subcellular localization of the receptor. For example, in the striatum: (1) lightly-labeled dendrites often gave rise to densely-labeled spines; (2) spines arising from labeled dendrites could be either labeled or unlabeled; and (3) label was sometimes seen in the spine neck but not in the spine head (Hersch et al., 1994). In addition, immunoperoxidase techniques are far more sensitive than immunogold techniques.

We also found very specific subcellular localization of M1R in our previous study of this receptor in the BLA using the V-VIP immunoperoxidase technique (Muller et al., 2013). For example, many M1R+ immunoparticles in excitatory and inhibitory axon terminals contacted the active zone of the presynaptic membrane, where they suggest presynaptic modulation of transmitter release by M1Rs (see Figs. 5 and 6 of Muller et al., 2013, and Figs. 4B and 4D of the present study). Thus, in the present study the localization of M1R+ immunoparticles in contact with or in close proximity to postsynaptic densities in spines receiving inputs from glutamatergic inputs suggests modulation of glutamatergic transmission by M1Rs in spines of BLA PNs. The V-VIP immunoperoxidase technique, however, is not as effective as immunogold techniques for discerning the ratio of membrane versus cytoplasmic receptors. For instance, in our studies of M2Rs in the BLA using the V-VIP technique (Muller et al., 2016) we found many spines that contained several immunoparticles, as in the present M1R study, but the immunogold-silver (IGS) technique was required to determine the percentage of M2R+ IGS particles that were membrane-associated in spines (62%), and thus in a position to be activated by acetylcholine (Fajardo-Serrano et al., 2017). Forty percent of the synaptic targets of cholinergic axon terminals in the BLA are spines, including many synaptic contacts with the necks of spines (Muller et al., 2011). Since the heads of these spines receive excitatory asymmetrical synapses from

glutamatergic terminals these cholinergic synapses are strategically positioned to modulate glutamatergic transmission via M1Rs (and M2Rs) in spines.

3.2 Origins of VGluT1+ and VGluT2+ inputs to the basolateral amygdala

In the present study approximately half of the spines receiving VGluT1+ inputs were M1R+ (Fig. 5). In situ hybridization studies have shown that VGluT1+ PN somata are found in all areas of the cerebral cortex and the basolateral amygdala (i.e., the cortex-like part of the amygdala) (Fremeau et al., 2001, 2004; Poulin et al., 2008). Thus, it is not clear whether there may be differential innervation of M1R+ spines in the BLA by VGluT1+ cortical PNs versus VGluT1+ local PNs in the BLA and other basolateral amygdalar nuclei which innervate BLA (Pitkänen et al., 1997; Pitkänen 2000). In the present study the great majority of targets of VGluT1+ terminals were spines, consistent with anterograde tract tracing studies of cortical afferents to the basolateral amygdala (Brinley-Reed et al., 1995; Farb and LeDoux, 1999) and intra-amygdalar PN to PN connections (Smith and Paré, 1994; Paré et al., 1995).

In the present study approximately half of the spines receiving VGluT2+ inputs were M1R+ (Fig. 5). VGluT2+ somata are mainly located in the diencephalon and brainstem (Fremeau et al., 2001; Kaneko and Fujiyama, 2002). The levels of VGluT2 mRNA are especially high in the midline and intralaminar thalamic nuclei, which have especially robust projections to the BLA (Turner and Herkenham, 1991; Vertes et al., 2006, 2008, 2012), but there is weak expression of VGluT2 in the hippocampal region, layers 4 and 6 of the neocortex, and the medial, cortical and anterior basomedial nuclei of the amygdala (Fremeau et al., 2001; Kaneko and Fujiyama, 2002; Poulin et al., 2008). Since the amygdalar nuclei with weak VGluT2+ expression have very limited projections to BLA, and the cortical projections to the BLA mainly arise from its superficial layers (layers 2 and 3), the contribution of these regions to the VGluT2+ axon terminal subpopulation in the BLA should be minimal. Likewise the VGluT1+ neurons in the hippocampus far outnumber the VGluT2+ neurons (Fremeau et al., 2001; Kaneko and Fujiyama, 2002). Given the massive input to basolateral amygdala from the VGluT2+ neurons in the midline and intralaminar thalamic nuclei, the great majority of VGluT2+ axon terminals seen in the present study undoubtedly represent inputs from the thalamus. The finding that only half of the VGluT2+ terminals synapse with M1R+ spines suggests the possibility that only some of the thalamic nuclei target M1R+ spines. In the present study the great majority of targets of VGluT2+ terminals in the BLA were spines, consistent with anterograde tract tracing studies of thalamic inputs to the basolateral amygdala (LeDoux et al., 1991; Farb and LeDoux, 1997; Radley et al., 2007).

3.3 A subset of VGluT1+ and VGluT2+ inputs to the basolateral amygdala express M1Rs

Although the main purpose of this study was to investigate the sources of different glutamatergic inputs to M1R+ spines, an ancillary finding was that some VGluT1+ and VGluT2+ axon terminals were themselves M1R+, and many targeted M1R+ spines. These were not consistently seen in our preparations, but only when the diffuse DAB reaction product for VGluTs was of light to moderate density and M1R+ immunoparticles were densely stained. This finding was not unexpected since a previous study found that many axon terminals in BLA forming asymmetrical synapses with spines were M1R+, and the

majority of the spines postsynaptic to these terminals were M1R+ (Muller et al., 2013). Although more consistent and more accurate determinations of the percentages of these terminals will require double-labeling techniques with more distinct reaction products, such as immunoperoxidase/immunogold techniques, these results suggest that acetylcholine can modulate glutamatergic inputs to BLA spines by presynaptic as well as postsynaptic M1R-mediated mechanisms. The presence of M1Rs on a subset of glutamatergic terminals in BLA is consistent with results from electrophysiological studies that have demonstrated modulation of glutamate release from axon terminals by M1R-mediated mechanisms. For example, Yajeya and coworkers used pirenzepine to block M1Rs and estimated that approximately 20% of the reduction in the amplitude of synaptically-evoked EPSPs in BLA pyramidal cells by carbachol was mediated by presynaptic M1Rs (Yajeya et al., 2000). Similarly, electrophysiology studies in our lab indicate that presynaptic M1Rs can contribute to the muscarine-induced suppression of both cortical and thalamic inputs to BLA pyramidal cells (Liu et al., 2012).

3.4 Functional implications

The expression of M1Rs in about half of the spines that are postsynaptic to VGluT1+ or VGluT2+ axon terminals suggests that these receptors could modulate glutamatergic input from both cortical and/or basolateral inputs, as well as thalamic inputs. The fact that PNs in the BLA and hippocampus share many structural and functional features, and that M1Rs are critical for mnemonic functions in both regions, suggests that M1R+ spines in both regions may function similarly. In the hippocampus M1R activation facilitates LTP by potentiating NMDAR currents (Markram and Segal, 1990; Shinoe et al., 2005; Buchanan and Mellor, 2010; Dennis et al., 2016) and this is correlated with colocalization of M1Rs and NMDARs in PN dendrites (Marino et al., 1998). Since the majority of NMDAR+ profiles in ultrastructural studies of BLA are spines (Farb et al., 1995), and the main targets of both cortical (Farb and LeDoux, 1997) and thalamic inputs (Farb and LeDoux, 1997; Radley et al., 2007) to the BLA are NMDAR+ spines, it is possible that a similar mechanism facilitates LTP involved in the formation of emotional memories in the BLA. In fact, there is evidence that interactions between NMDARs and muscarinic receptors in the BLA are critical for the retrieval of emotional memories (Nazarinia et al., 2016). However, additional dual-labeling M1R/NMDAR immunohistochemical investigations at the ultrastructural level, as well as functional studies, will be required to determine if interactions between M1Rs and NMDARs facilitate LTP involved in the formation of emotional memories in the BLA.

4. Experimental procedures

4.1 Animals

Experiments were performed using a total of 6 male B6129SF2/J mice (8–12 weeks old; Jackson Laboratory, Bar Harbor, Me). All animals were housed on a 12-h light/dark cycle with ad libitum access to food and water. All experiments were carried out in accordance with the National Institutes of Health Guide for the Care and Use of Laboratory Animals and were approved by the Institutional Animal Use and Care Committee (IACUC) of the University of South Carolina. All efforts were made to minimize animal suffering and to use the minimum number of animals necessary to produce reliable scientific data.

4.2 Tissue preparation for dual-labeling immunoelectron microscopy

Mice were deeply anesthetized with isoflurane and perfused intracardially with phosphate buffered saline (PBS; pH 7.4) containing 0.5% sodium nitrite (50 ml) followed by an acrolein/paraformaldehyde mixture (2.0% paraformaldehyde-3.75% acrolein in 0.1 M phosphate buffer (PB; pH 7.4) for 1 minute, followed by 2.0% paraformaldehyde in PB for 20 minutes. Following removal, brains were postfixed in 2.0% paraformaldehyde in PB for 1 h and sectioned on a vibratome in the coronal plane at 60 μ m. Sections were rinsed in 1.0% borohydride in PB for 30 m and then rinsed thoroughly in several changes of PB for 1h. They were then processed for immunocytochemistry in the wells of tissue culture plates.

Amygdalas from three brains were processed for electron microscopic immunocytochemistry using a sequential, pre-embedding, dual-labeling immunoperoxidase method (Muller et al., 2006). Electron microscopic analysis was performed to determine the extent to which excitatory VGluT1 or VGluT2 immunoreactive axon terminals were presynaptic to MIR immunoreactive dendritic spines in the anterior subdivision of the basolateral nucleus (BLa; bregma levels -0.1 through -1.3 ; Paxinos and Franklin, 2013). BLa was chosen for study because it receives the densest cholinergic innervation in the amygdala, and since MIRs in the BLa are known to be critical for memory consolidation of emotionally arousing experiences (McGaugh, 2004).

Sections through the BLa were first incubated at room temperature in a blocking solution containing 2% normal goat serum, 1% bovine serum albumin, and 0.04% Triton-X 100 in PBS for 1 h. This solution also served as a diluent for primary and secondary antibodies. Sections were then processed using a rabbit polyclonal antibody to MIR (1:2000; Sigma Chemical Company, St. Louis, MO) for 2 days at 4° C, a biotinylated goat anti-rabbit secondary antibody for 1 h at room temperature (1:200; Vector Laboratories, Burlingame, CA), and a Vectastain Elite ABC kit (Vector Laboratories, Burlingame, CA). MIR immunoreactivity was then visualized using a Vector VIP (Very Intense Purple) peroxidase substrate kit (Vector Laboratories). This procedure yields a reaction product that appears purple in the light microscope, and granular or particulate in the electron microscope (Van Haefen and Wouterlood, 2000; Muller et al., 2006). After rinsing, sections were incubated in an avidin/biotin blocking solution (Avidin/Biotin Blocking Kit, Vector Laboratories). Sections were then incubated for 16 hrs at 4°C in either a guinea pig anti-VGluT1 antibody (1:10,000; Millipore, Burlingame, MA) or a mouse anti-VGluT2 antibody (1:1500; Millipore), and then in biotinylated goat anti-guinea pig or goat anti-mouse secondary antibodies (1:200; Vector Laboratories) for 1 h at room temperature, and then processed using a Vectastain Standard ABC kit (Vector Laboratories) with DAB (3, 3'-diaminobenzidine-4HCl, Sigma) as a chromogen to produce a brown reaction product. At the ultrastructural level the diffuse DAB immunoperoxidase reaction product was easily distinguishable from the particulate V-VIP immunoperoxidase reaction product. Controls sections were processed with one of the primary antibodies omitted.

Sections were then postfixed in 2% osmium tetroxide in 0.01M PBS (pH 7.4) for 1 h, dehydrated in graded ethanols and acetone, and flat embedded in Polybed 812 (Polysciences, Warrington, PA) between sheets of Aclar (Ted Pella, Redding, CA). Silver thin-sections were cut on an ultramicrotome (Ultracut R, Leica, Germany), collected on

formvar-coated copper grids, stained with uranyl acetate and lead citrate, and examined with a JEOL-1400 Plus Transmission electron microscope (JEOL, Tokyo, Japan).

4.2 Ultrastructural analysis

One or two vibratome sections were chosen from each brain for each neurochemical combination (M1R/VGluT1 and M1R/VGluT2) for quantitative ultrastructural analysis. In each thin section, areas near the tissue/resin interface that exhibited both M1R and VGluT immunoreactivity were analyzed. Somata, dendritic shafts, dendritic spines, axons, axon terminals, and synapses were identified using established morphological criteria (Peters et al., 1991). In M1R/VGluT1 preparations VGluT1-immunoreactive (VGluT1+) axon terminals forming synapses with spines were identified and then analyzed to determine if their postsynaptic spines were M1R+. An analogous sampling technique was used for M1R/VGluT2. Light and electron microscopic examination of sections processed using this dual-labeling V-VIP/DAB immunoperoxidase method, but with the VGluT primary antibodies omitted, produced no DAB-labeled axon terminals. Sections processed with the M1R primary antibodies omitted produced very few V-VIP immunoparticles, but occasional single particles were seen in some structures, including spines. For this reason, as a conservative measure, only spines with 2 or more V-VIP immunoparticles were considered to be M1R+. In each brain counts were made to determine the percentage of VGluT1+ and VGluT2+ terminals that formed synapses with M1R+ versus M1R-negative spines.

4.3 Tissue preparation for light microscopy

Prior to the electron microscopic studies amygdalas from three brains were used for light microscopic immunohistochemistry, including trials to determine appropriate antibody dilutions. The same immunohistochemical procedures used for the electron microscopic studies were employed, except the sections were not osmicated and embedded for electron microscopy. Some sections were processed for light microscopic single-labeling of M1R, VGluT1, and VGluT2 using the same chromogens used in the electron microscopic study, whereas others were processed for light microscopic M1R/VGluT1 and M1R/VGluT2 double-labeling using the same chromogens used in the electron microscopic study. Following immunohistochemical processing, sections were mounted on gelatinized slides, dried overnight, dehydrated in ascending alcohols, cleared in xylene, and coverslipped with Permount (Fisher). Sections were analyzed using an Olympus BX51 microscope and digital light micrographs were taken with an Olympus DP2-BSW camera system.

4.4 Primary Antibody Specificity

The polyclonal M1R antibody (Sigma-Aldrich Cat# M9808, RRID:AB_260731) was raised in rabbit to a highly purified GST fusion protein of a part of the third intracellular loop of the human m1 receptor corresponding to amino acids 227–353. This part of the third intracellular loop shows virtually no sequence homology with other muscarinic receptor subtypes, but is homologous between species (Bonner et al., 1987). The specificity of this antibody for M1R has been previously established (Levey et al., 1991). Immunoblotting demonstrated a protein band that was distinct from other muscarinic receptor subtypes. Immunoprecipitation experiments demonstrated that this antiserum only bound the M1R

receptor subtype. Preadsorption of the antiserum with the third intracellular loop fusion protein blocked antibody binding.

The polyclonal VGluT1 antibody (Millipore Cat# AB5905, RRID:AB_2301751) was raised in guinea pig to a synthetic peptide from rat VGluT1 protein with no overlap with VGluT2. It recognizes the expected single ca. 60 kDa band on Western blots (Melone et al., 2005). Double labeling studies using this and other VGluT1 antibodies have demonstrated virtually complete overlap of immunostaining in the rodent brain (Melone et al., 2005; Graziano et al., 2008). Preadsorption with the immunogen peptide eliminates all staining (manufacturer's technical information).

The monoclonal VGluT2 antibody (Millipore Cat# MAB5504, RRID:AB_2187552) was raised in mouse to recombinant protein from rat VGluT2. This antibody stained a single band of 56 kDa molecular weight in Western blots of mouse brain lysates (manufacturer's technical information) as well as a single band of 56 kDa molecular weight in Western blots from macaque cerebellar tissue (Balaram et al., 2013).

Acknowledgements

We greatly appreciate the excellent technical assistance of Jeffrey Davis of the USC School of Medicine Instrumentation Resource Facility (IRF) in the processing of tissue for electron microscopy.

Funding statement

This work was supported by the National Institutes of Health Grant R01MH104638.

Abbreviations

BLa	anterior subdivision of the basolateral amygdalar nucleus
DAB, 3	3'-diaminobenzidine-4HCl
M1R	type 1 muscarinic receptor
M2R	type 2 muscarinic receptor
NMDAR	NMDA glutamate receptor
PN	pyramidal neuron
VGluT1	type 1 vesicular glutamate transporter protein
VGluT2	type 2 vesicular glutamate transporter protein
V-VIP	Vector Very Intense Purple

References

Balaram P, Hackett TA, Kaas JH, 2013 Differential expression of vesicular glutamate transporters 1 and 2 may identify distinct modes of glutamatergic transmission in the macaque visual system. *J Chem Neuroanat.* 50–51, 21–38.

- Boccia MM, Blake MG, Baratti CM, McGaugh JL 2009 Involvement of the basolateral amygdala in muscarinic cholinergic modulation of extinction memory consolidation. *Neurobiol Learn Mem.* 91,93–97. [PubMed: 18706510]
- Bonner TI, Buckley NJ, Young AC, Brann MR 1987 Identification of a family of muscarinic acetylcholine receptor genes. *Science* 237, 527–532. [PubMed: 3037705]
- Brinley-Reed M, Mascagni F, McDonald AJ 1995 Synaptology of prefrontal cortical projections to the basolateral amygdala: an electron microscopic study in the rat. *Neuroscience Lett.* 202, 45–48.
- Carlsen J, Zaborszky L, Heimer L 1985 Cholinergic projections from the basal forebrain to the basolateral amygdaloid complex: a combined retrograde fluorescent and immunohistochemical study. *J. Comp. Neurol* 234,155–167. [PubMed: 3886715]
- Dennis SH, Pasqui F, Colvin EM, Sanger H, Mogg AJ, Felder CC, Broad LM, Fitzjohn SM, Isaac JT, Mellor JR 2016 Activation of muscarinic m1 acetylcholine receptors induces long-term potentiation in the hippocampus. *Cereb Cortex* 26, 414–426. [PubMed: 26472558]
- Farb CR, Aoki C, LeDoux JE 1995 Differential localization of NMDA and AMPA receptor subunits in the lateral and basal nuclei of the amygdala: a light and electron microscopic study. *J Comp Neurol.* 362, 86–108. [PubMed: 8576430]
- Fajardo-Serrano A, Liu L, Mott DD, McDonald AJ 2017 Evidence for M2 muscarinic receptor modulation of axon terminals and dendrites in the rodent basolateral amygdala: an ultrastructural and electrophysiological analysis. *Neuroscience* 357, 349–362. [PubMed: 28629847]
- Farb CR, LeDoux JE 1997 NMDA and AMPA receptors in the lateral nucleus of the amygdala are postsynaptic to auditory thalamic afferents. *Synapse* 27, 106–121. [PubMed: 9266772]
- Farb CR, LeDoux JE 1999 Afferents from rat temporal cortex synapse on lateral amygdala neurons that express NMDA and AMPA receptors. *Synapse* 33, 218–229. [PubMed: 10420169]
- Fremeau RT Jr., Troyer MD, Pahner I, Nygaard GO, Tran CH, Reimer RJ, Bellocchio EE, Fortin D, Storm-Mathisen J, Edwards RH 2001 The expression of vesicular glutamate transporters defines two classes of excitatory synapse. *Neuron* 31, 247–260. [PubMed: 11502256]
- Graziano A, Liu XB, Murray KD, Jones EG 2008 Vesicular glutamate transporters define two sets of glutamatergic afferents to the somatosensory thalamus and two thalamocortical projections in the mouse. *J Comp Neurol.* 507, 1258–1276. [PubMed: 18181146]
- Hershey SM, Gutekunst CA, Rees HD, Heilman CJ, Levey AI 1994 Distribution of m1–m4 muscarinic receptor proteins in the rat striatum: light and electron microscopic immunocytochemistry using subtype-specific antibodies. *J Neurosci.* 14(5 Pt 2), 3351–3363. [PubMed: 8182478]
- Humeau Y, Herry C, Kemp N, Shaban H, Fourcaudot E, Bissière S, Lüthi A 2005 Dendritic spine heterogeneity determines afferent-specific Hebbian plasticity in the amygdala. *Neuron* 45, 119–131. [PubMed: 15629707]
- Kaneko T, Fujiyama F 2002 Complementary distribution of vesicular glutamate transporters in the central nervous system. *Neurosci Res.* 42, 243–250. [PubMed: 11985876]
- Kordower JH, Bartus RT, Marciano FF, Gash DM 1989 Telencephalic cholinergic system of the New World monkey (*Cebus apella*): morphological and cytoarchitectonic assessment and analysis of the projection to the amygdala. *J Comp Neurol.* 279, 528–545. [PubMed: 2465322]
- LeDoux JE, Farb CR, Milner TA 1991 Ultrastructure and synaptic associations of auditory thalamo-amygdala projections in the rat. *Exp Brain Res* 85, 577–586. [PubMed: 1717305]
- Lee S, Amir A, Pare J, Jenkins S, Pare D, Smith Y 2017 Is vGluT2 a universal marker of thalamic terminals? Program No. 757.11 2017 Neuroscience Meeting Planner. Washington DC: Society for Neuroscience, 2017 Online.
- Levey AI, Kitt CA, Simonds WF, Price DL, Brann MR 1991 Identification and localization of muscarinic acetylcholine receptor proteins in brain with subtype-specific antibodies. *J Neurosci.* 11, 3218–3226. [PubMed: 1941081]
- Liu L, McDonald AJ, Mott DD 2012 Muscarinic modulation of glutamatergic neurotransmission in the basolateral amygdala. Program No. 143.06. 2012 Neuroscience Meeting Planner. New Orleans, LA: Society for Neuroscience, 2012 Online.
- Marino MJ, Rouse ST, Levey AI, Potter LT, Conn PJ 1998 Activation of the genetically defined m1 muscarinic receptor potentiates N-methyl-D-aspartate (NMDA) receptor currents in hippocampal pyramidal cells. *Proc Natl Acad Sci U S A.* 95, 11465–11470. [PubMed: 9736760]

- Markram H, Segal M 1990 Long-lasting facilitation of excitatory postsynaptic potentials in the rat hippocampus by acetylcholine. *J Physiol.* 427, 381–393. [PubMed: 2145426]
- McDonald AJ 1982 Neurons of the lateral and basolateral amygdaloid nuclei: a Golgi study in the rat. *J. Comp. Neurol* 212, 293–312. [PubMed: 6185547]
- McDonald AJ, Mascagni F 2010 Neuronal localization of m1 muscarinic receptor immunoreactivity in the rat basolateral amygdala. *Brain Struct. Funct* 215, 37–48. [PubMed: 20503057]
- McDonald AJ, 2019 Functional neuroanatomy of the basolateral amygdala: neurons, neurotransmitters, and circuits, in: Urban J and Rosenkranz A (Eds.), *Handbook of Amygdala Structure and Function*. Elsevier, Amsterdam, In Press.
- McGaugh JL 2004 The amygdala modulates the consolidation of memories of emotionally arousing experiences. *Annu Rev Neurosci.* 27, 1–28. [PubMed: 15217324]
- Melone M, Burette A, Weinberg RJ 2005 Light microscopic identification and immunocytochemical characterization of glutamatergic synapses in brain sections. *J Comp Neurol.* 492, 495–509. [PubMed: 16228991]
- Mesulam MM, Mufson EJ, Wainer BH, Levey AI 1983a Central cholinergic pathways in the rat: an overview based on an alternative nomenclature (Ch1-Ch6). *Neuroscience* 10, 1185–1201. [PubMed: 6320048]
- Mesulam MM, Mufson EJ, Levey AI, Wainer BH 1983b Cholinergic innervation of cortex by the basal forebrain: cytochemistry and cortical connections of the septal area, diagonal band nuclei, nucleus basalis (substantia innominata), and hypothalamus in the rhesus monkey. *J Comp Neurol.* 214, 170–197. [PubMed: 6841683]
- Millhouse OE, DeOlmos J 1983 Neuronal configurations in lateral and basolateral amygdala. *Neuroscience* 10, 1269–1300. [PubMed: 6664494]
- Mrzljak L, Levey AI, Goldman-Rakic PS 1993 Association of m1 and m2 muscarinic receptor proteins with asymmetric synapses in the primate cerebral cortex: morphological evidence for cholinergic modulation of excitatory neurotransmission. *Proc Natl Acad Sci U S A.* 90, 5194–5198. [PubMed: 8389473]
- Muller JF, Mascagni F, McDonald AJ 2006 Pyramidal cells of the rat basolateral amygdala: Synaptology and innervation by parvalbumin-immunoreactive interneurons. *J. Comp. Neurol* 494, 635–650. [PubMed: 16374802]
- Muller JF, Mascagni F, McDonald AJ 2011 Cholinergic innervation of pyramidal cells and interneurons in the rat basolateral amygdala. *J. Comp. Neurol* 519, 790–805. [PubMed: 21246555]
- Muller JF, Mascagni F, Zaric V, McDonald AJ (2013) Muscarinic cholinergic receptor M1 in the rat basolateral amygdala: ultrastructural localization and synaptic relationships to cholinergic axons. *J Comp Neurol.* 521:1743–1759. [PubMed: 23559406]
- Muller JF, Mascagni F, Zaric V, Mott DD, McDonald AJ 2016 Localization of the m2 muscarinic cholinergic receptor in dendrites, cholinergic terminals and non-cholinergic terminals in the basolateral amygdala: An ultrastructural analysis. *J Comp Neurol.* 524, 2400–2417. [PubMed: 26779591]
- Nazarinia E, Rezayof A, Sardari M, Yazdanbakhsh N 2017 Contribution of the basolateral amygdala NMDA and muscarinic receptors in rat's memory retrieval. *Neurobiol Learn Mem.* 139, 28–36. [PubMed: 27993648]
- Paré D, Smith Y, Paré JF 1995 Intra-amygdaloid projections of the basolateral and basomedial nuclei in the cat: Phaseolus vulgaris-leucoagglutinin anterograde tracing at the light and electron microscopic level. *Neuroscience* 69, 567–583. [PubMed: 8552250]
- Paxinos G, Franklin K, 2013 *The Mouse Brain in Stereotaxic Coordinates*, fourth ed Academic Press, Cambridge Massachusetts.
- Peters A, Palay SL, Webster HD 1991 *The fine structure of the nervous system*. Oxford University Press, New York.
- Petralia RS, Yokotani N, Wenthold RJ 1994 Light and electron microscope distribution of the NMDA receptor subunit NMDAR1 in the rat nervous system using a selective anti-peptide antibody. *J Neurosci.* 14, 667–96. [PubMed: 8301357]
- Pitkänen A 2000 Connectivity of the rat amygdala, in *The Amygdala*, second edition, Aggleton JP, (Ed), pp. 31–116. Oxford University Press, Oxford.

- Pitkänen A, Savander V, LeDoux JE 1997 Organization of intra-amygdaloid circuitries in the rat: an emerging framework for understanding functions of the amygdala. *Trends Neurosci* 20, 517–523. [PubMed: 9364666]
- Poulin JF, Castonguay-Lebel Z, Laforest S, Drolet G 2008 Enkephalin co-expression with classic neurotransmitters in the amygdaloid complex of the rat. *J Comp Neurol*. 506, 943–959. [PubMed: 18085591]
- Power AE, Vazdarjanova A, McGaugh JL 2003a Muscarinic cholinergic influences in memory consolidation. *Neurobiol Learn Mem*. 80, 178–193. [PubMed: 14521862]
- Power AE, McIntyre CK, Litmanovich A, McGaugh JL 2003b Cholinergic modulation of memory in the basolateral amygdala involves activation of both m1 and m2 receptors. *Behav Pharmacol*. 14, 207–213. [PubMed: 12799522]
- Radley JJ, Farb CR, He Y, Janssen WG, Rodrigues SM, Johnson LR, Hof PR, LeDoux JE, Morrison JH 2007 Distribution of NMDA and AMPA receptor subunits at thalamo-amygdaloid dendritic spines. *Brain Res*. 1134, 87–94. [PubMed: 17207780]
- Rouse ST, Gilmor ML, Levey AI 1998 Differential presynaptic and postsynaptic expression of m1–m4 muscarinic acetylcholine receptors at the perforant pathway/granule cell synapse. *Neuroscience* 86:221–232. [PubMed: 9692756]
- Shinoe T, Matsui M, Taketo MM, Manabe T 2005 Modulation of synaptic plasticity by physiological activation of M1 muscarinic acetylcholine receptors in the mouse hippocampus. *J Neurosci*. 25, 11194–11200. [PubMed: 16319319]
- Smith Y, Paré D 1994 Intra-amygdaloid projections of the lateral nucleus in the cat: PHA-L anterograde labeling combined with postembedding GABA and glutamate immunocytochemistry. *J Comp Neurol*. 342:232–248. [PubMed: 7911130]
- Turner BH, Herkenham M 1991 Thalamoamygdaloid projections in the rat: a test of the amygdala's role in sensory processing. *J. Comp. Neurol* 313, 295–325. [PubMed: 1765584]
- Van Haeften T, Wouterlood FG 2000 Neuroanatomical tracing at high resolution. *J Neurosci Methods* 103, 107–116. [PubMed: 11074100]
- Vertes RP, Hoover WB, Do Valle AC, Sherman A, Rodriguez JJ 2006 Efferent projections of reuniens and rhomboid nuclei of the thalamus in the rat. *J Comp Neurol* 499, 768–796. [PubMed: 17048232]
- Vertes RP, Hoover WB 2008 Projections of the paraventricular and paratenial nuclei of the dorsal midline thalamus in the rat. *J Comp Neurol*. 508, 212–237. [PubMed: 18311787]
- Vertes RP, Hoover WB, Rodriguez JJ 2012 Projections of the central medial nucleus of the thalamus in the rat: node in cortical, striatal and limbic forebrain circuitry. *Neuroscience* 19, 120–136.
- Yajeya J, De La Fuente A, Criado JM, Bajo V, Sánchez-Riolobos A, Heredia M 2000 Muscarinic agonist carbachol depresses excitatory synaptic transmission in the rat basolateral amygdala in vitro. *Synapse* 38,151–160. [PubMed: 11018789]

Highlights

- Glutamatergic inputs to the basolateral amygdala (BLa) mainly target spines
- Half of these spines express the type 1 muscarinic receptor (M1R)
- Half of the spines targeted by both VGluT1+ or VGluT2+ axon terminals are M1R+
- A subset of VGluT1+ and VGluT2+ axon terminals express M1Rs
- Thus, diverse glutamatergic inputs to BLa spines may be modulated by M1Rs

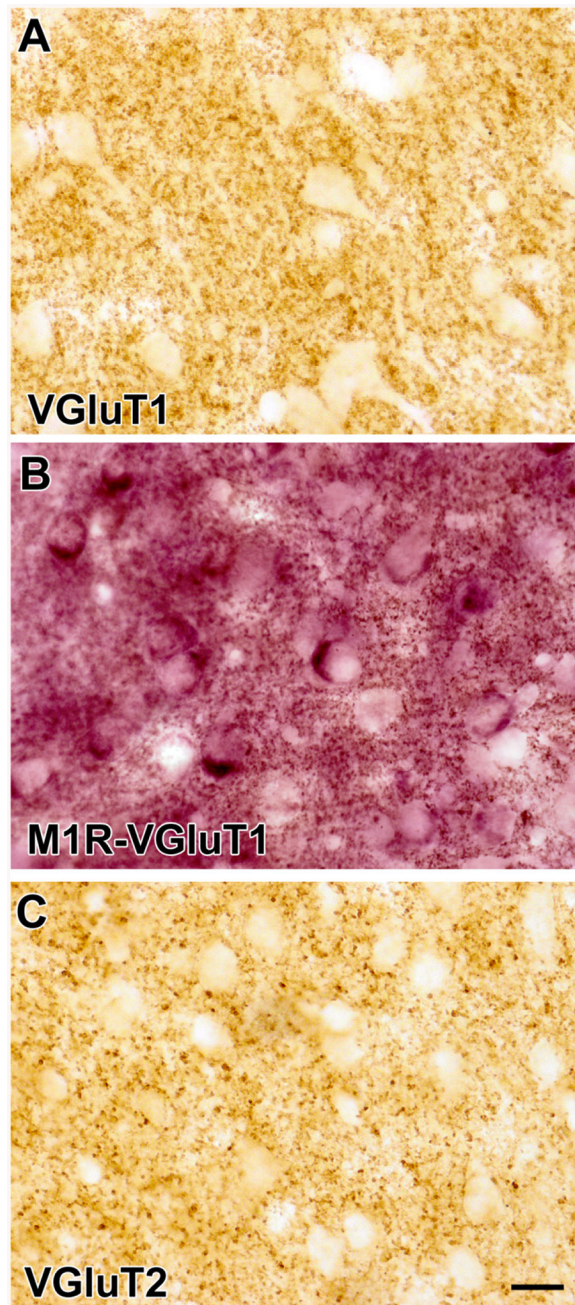


Figure 1. (A) Photomicrograph of VGlut1 immunoreactivity in the BLA (DAB immunoperoxidase). Note that neuronal somata and proximal dendrites are unlabeled but there are punctate VGlut1+ axons and axon terminals in the neuropil. (B) Photomicrograph of a section stained for M1R with V-VIP as a chromogen in the BLA. Note that somata of putative PNs are stained purple. This section was also stained for VGlut1 immunoreactivity with DAB as a chromogen. The neuropil contains small punctate structures that represent VGlut1+ axons and M1R+ processes. (C) Photomicrograph of VGlut2 immunoreactivity in the BLA (DAB immunoperoxidase). Note that somata and proximal dendrites are unlabeled but there are

punctate VGluT2+ axons and axon terminals in the neuropil. Scale bar = 20 μ m for A, B, and C.

Author Manuscript

Author Manuscript

Author Manuscript

Author Manuscript

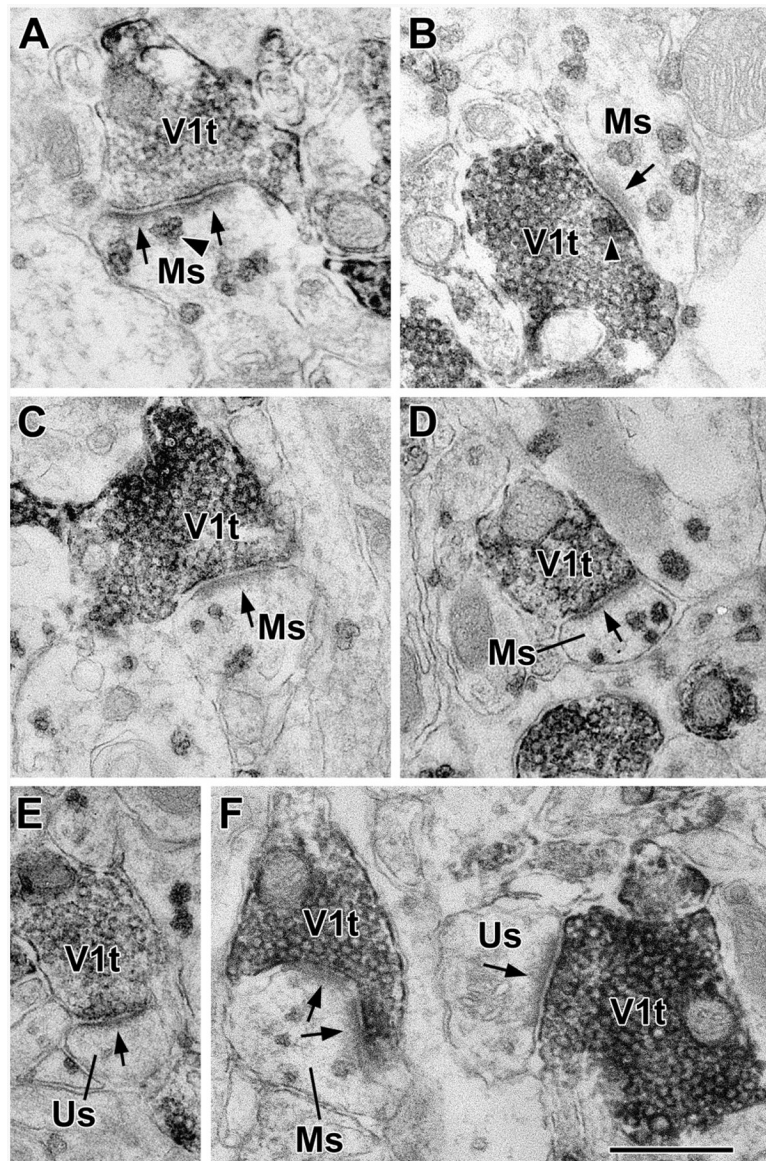


Figure 2. VGlut1+ axon terminals (V1t) form asymmetrical synapses with M1R+ spines (Ms) and unlabeled M1R-negative spines (Us) in the BLA. (A) A VGlut1+ terminal forms an asymmetrical synapse with an M1R+ spine. Arrows indicate postsynaptic densities in this and all other electron micrographs. An arrowhead indicates a representative M1R+ particle near the postsynaptic densities. There are four more M1R+ particles in this spine. (B) A VGlut1+ terminal forms an asymmetrical synapse with an M1R+ spine. There is also an M1R+ particle in the terminal at the active zone of the presynaptic membrane (arrowhead). (C and D) VGlut1+ terminals form asymmetrical synapses with M1R+ spines. (E) A VGlut1+ terminal forms an asymmetrical synapse with an unlabeled spine. (F) VGlut1+ terminals form asymmetrical synapses with an M1R+ spine (left) and an unlabeled spine (right). Scale bar = 500 nm.

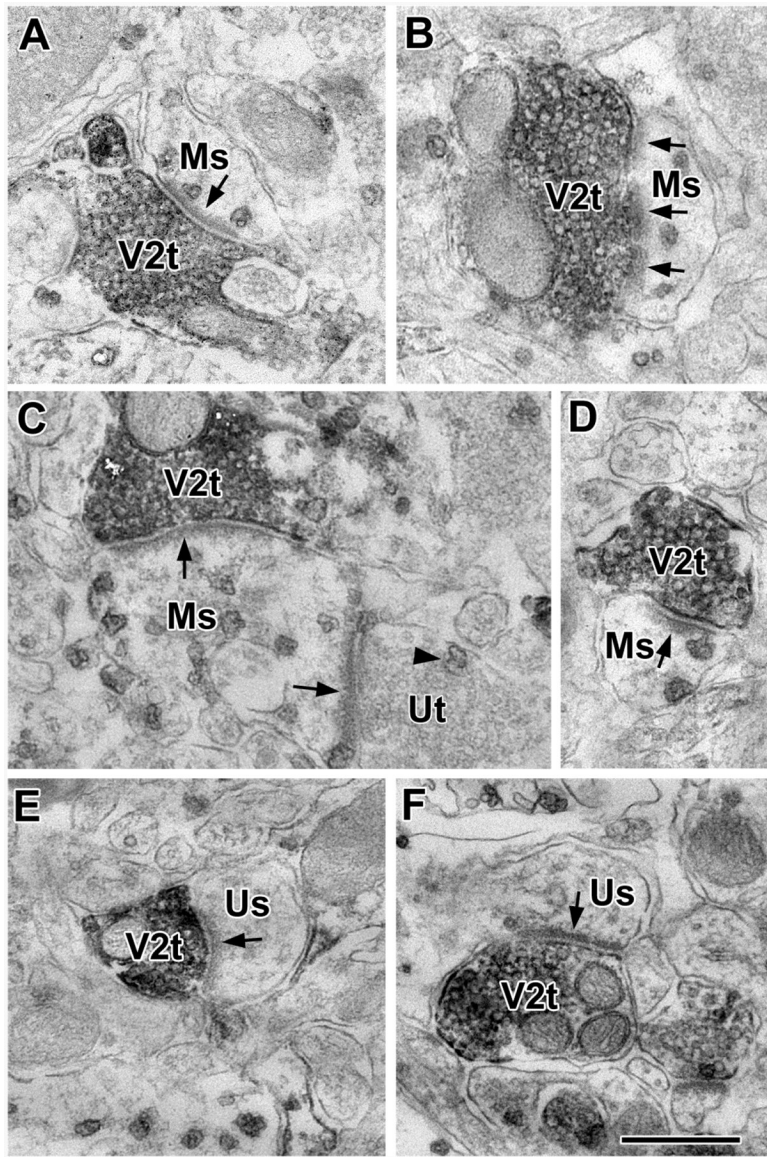


Figure 3. VGluT2+ axon terminals (V2t) form asymmetrical synapses with M1R+ spines (Ms) and unlabeled M1R-negative spines (Us) in the BLA. (A and B) VGluT2+ terminals form asymmetrical synapses with M1R+ spines. (C) A large M1R+ spine is postsynaptic to a VGluT2+ terminal and an unlabeled terminal (Ut). The unlabeled terminal contains one M1R+ particle. (D) A VGluT2+ terminal forms an asymmetrical synapse with an M1R+ spine. (E and F) VGluT2+ terminals form asymmetrical synapses with unlabeled spines. Scale bar = 500 nm.

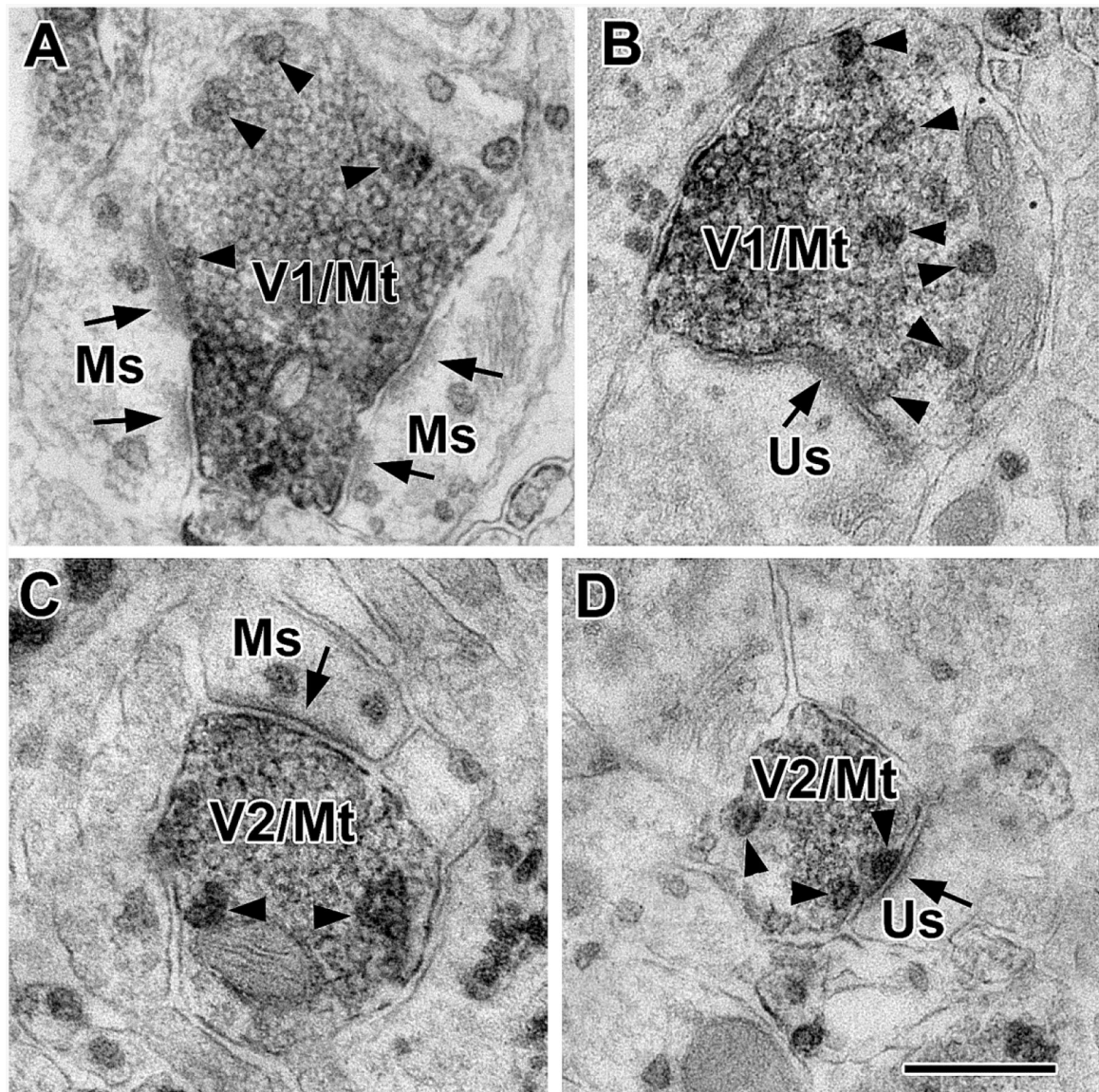


Figure 4. Terminals immunoreactive for both VGluT1 and M1R (V1/Mt) and terminals immunoreactive for both VGluT2 and M1R (V2/Mt) form asymmetrical synapses with M1R + spines (Ms) and unlabeled M1R-negative spines (Us) in the BLA. Arrowheads indicate M1R+ particles in terminals. (A) A VGluT1/M1R double-labeled terminal forms asymmetrical synapses with two M1R+ spines. (B) A VGluT1/M1R double-labeled terminal forms an asymmetrical synapses with an unlabeled spine. (C) A VGluT2/M1R double-labeled terminal forms an asymmetrical synapse with an M1R+ spine. (D) A VGluT2/M1R double-labeled terminal forms an asymmetrical synapse with an unlabeled spine. Scale bar = 500 nm.

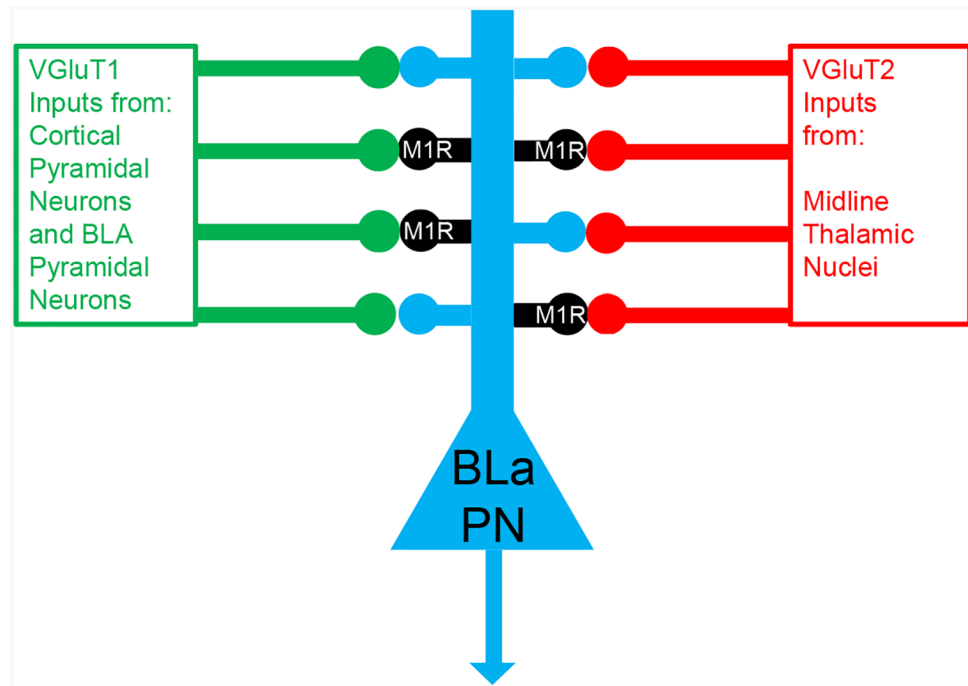


Figure 5. Schematic Diagram illustrating the main results of the present study, namely that about half of all cortical/BLA inputs and thalamic inputs to spines of BLA pyramidal neurons (PN) synapse with M1R+ spines.

Table 1.

Percentages of VGluT1+ and VGluT2+ axon terminals that synapse with M1R+ spines.

Brain	VGluT1 synapses with M1R+ spines	VGluT2 synapses with M1R+ spines
M7	47.4% (45/92)	51.6% (48/93)
M10	44.7% (42/94)	40.8% (31/76)
M12	55.5% (50/90)	50.0% (42/84)
Total	49.6% (137/276)	47.8% (121/253)

Author Manuscript

Author Manuscript

Author Manuscript

Author Manuscript